AIP | Applied Physics Letters

Controlled movement of superparamagnetic bead rows for microfluid mixing

Dennis Holzinger, Daniel Lengemann, Florian Göllner, Dieter Engel, and Arno Ehresmann

Citation: Applied Physics Letters **100**, 153504 (2012); doi: 10.1063/1.3701723
View online: http://dx.doi.org/10.1063/1.3701723
View Table of Contents: http://scitation.aip.org/content/aip/journal/apl/100/15?ver=pdfcov
Published by the AIP Publishing

Controlled movement of superparamagnetic bead rows for microfluid mixing

Dennis Holzinger, Daniel Lengemann, Florian Göllner, Dieter Engel, and Arno Ehresmann
Institute of Physics and Center for Interdisciplinary Nanostructure Science and Technology, University of Kassel, Heinrich-Plett-Str. 40, D-34132 Kassel, Germany

(Received 8 December 2011; accepted 17 March 2012; published online 9 April 2012)

The controlled movement of magnetic beads trapped on a surface in the moving inhomogeneous stray fields of moving domain walls between artificial domains of exchange bias layer systems has been applied for mixing of two aqueous fluids in a microfluidic device of small volume. The mixing of the two fluids can be considerably accelerated by transporting full rows of beads and use them as micro stirrers. The mixing speed in the current experiment is tripled in the first 6 min of mixing as compared to normal diffusion even for ratios of 250 between container height and bead diameter. © *2012 American Institute of Physics*. [http://dx.doi.org/10.1063/1.3701723]

The development of efficient mixing in microfluidic systems is an active field of research due to increasing demands in *Lab-on-a-chip* (LOC) concepts or *micro-total analysis systems* (μTASs) for biological, chemical, medical, and pharmaceutical applications.[1–3] In these devices, smallest amounts of fluids must be controlledly transported and for many applications mixed.[4]

However, mixing of two fluids in a microfluidic container is dominated by slow molecular diffusion at the interface between the different fluids[5,6] due to the small Reynolds number R_e leading to laminar flows and an increasing fraction of the fluid volume adhering to the walls when container dimensions are reduced. Hence, efficient mixing can only be achieved by increasing the contact interface between the fluids[6] or by disturbing the wall adhesion layer. One way to increase the mixing efficiency is active mixing, where external energy is transferred into the mixing device via electric or magnetic fields, ultrasound and miniaturized impellers, or micro nozzles.[7–9] For active mixing, the use of controlledly moving superparamagnetic beads for stirring is extremely promising,[10,11] if it is possible to achieve controlled particle movement of a large number of particles and if it is possible to avoid clustering of the magnetic beads close to or on container walls. Due to the superparamagnetic particle movement, both the mobility of the fluid lamellae and the interface is increased; hence, the mixing efficiency is enhanced.

However, forces on superparamagnetic particles by magnetic gradient fields from usual laboratory field sources are weak, and achievable steady state velocities far away from surfaces are rather slow. Moreover, if the particles are close to one of the container walls, the weak magnetic forces will not be able to overcome the surface-particle sticking forces DLVO (Derjaguin, Landau, Verwey, Overbeek) forces[12], and therefore these particles will not move.[13] Therefore, to avoid sticking, several techniques have been developed, mainly based on chemical modifications of either substrate or particles[14–17] or both.

Here we show an implementation of magnetic field induced active mixing by the controlled movement of commercially available superparamagnetic beads over a surface trapped in designed moving domain walls without chemical modification of bead or substrate. The principle of particle movement has recently been demonstrated to work without any further measures for surface coating, using an exchange bias (EB) layer system artificially patterned into magnetic parallel-stripe domains as a substrate.[13] Designed parallel-stripe domains with adjustable widths in the range of 2–10 μm have been prepared by a combination of lithography and keV He^+-ion bombardment with average remanent magnetizations perpendicular to the long stripe axes and antiparallel in adjacent stripes (Fig. 1).[18,19] Such a domain pattern maximizes the stray fields' gradients over domain walls,[20–22] inducing maximum forces attracting superparamagnetic beads to the surface. Since magnetic moments of superparamagnetic particles align parallel in the field of one domain wall, beads trapped in one domain wall repel each other, avoiding clustering by orders of magnitude. With a special field pulse, domain walls in such a substrate can be moved in predefined directions, thereby moving particles trapped in the corresponding stray fields.[13]

In the present paper, we will show experimentally that the controlled movement of superparamagnetic bead rows trapped in the moving stray fields of moving domain walls (domain wall movement assisted transport, DOWMAT) enhances the mixing speed in a microfluidic device between two different fluids as a proof of principle.

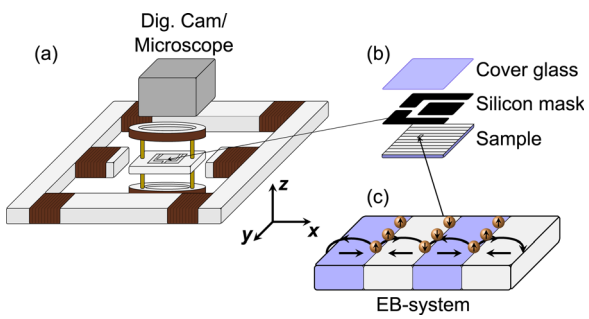

FIG. 1. (a) Schematic view of the experimental setup. The aperture in the top-coil enables observation either by an optical microscope or a digital camera. The mixing chamber consists of the substrate with designed parallel-stripe domains covered by a silicon mask with a thickness of 500 μm and is top-closed by a cover glass. (b) The two fluid injection channels are seen at the right hand side of the mask. (c) illustrates the magnetically stripe patterned EB-system: the average remanent magnetizations within the stripe domains are indicated by the antiparallel oriented arrows in adjacent stripes. The stray fields are sketched as curved arrows. Superparamagnetic beads (spheres) are attracted and magnetically aligned by the stray fields.

The fluid mixing chamber has been fabricated using silicon for the fluid channels placed on top of the magnetically patterned substrate (Fig. 1). The silicon mask had a thickness of 500 μm, was top-closed by a cover glass, and mechanically compacted. The EB layer system of the substrate was $Ta^{5\,nm}/Ru^{2\,nm}/IrMn^{12\,nm}/NiFe^{7.5\,nm}/Ta^{5\,nm}$, prepared by dc magnetron sputtering on a naturally oxidized silicon etch substrate, possessing an initial EB-field of $H_{EB,i} = 14.7$ kA/m. The substrate had a quadratic shape with an edge length of 1.5 cm. Artificial magnetic 5 μm wide parallel stripe domains were fabricated by ion bombardment induced magnetic patterning (IBMP),[18,19] using 10 keV He ion bombardment (ion dose: 5×10^{14} ions/cm^2) in an applied in-plane magnetic field H_{IB} of 80 kA/m, with average $H_{EB,i}$ directions antiparallel in adjacent stripes and perpendicular to the long stripe axes. The RMS surface roughness after magnetic patterning has been determined by atomic force microscopy to be about 1 nm.

The fluid chamber has been inserted into a home built electro magnet for tailored magnetic field pulses in x-direction and a pair of coils for field pulses in z-direction (see Fig. 1). The field pulse scheme is depicted in Fig. 2(a) consisting of double pulses with x- and z-field components with individual pulse lengths Δt_{pl} of 0.2 s and periodicities Δt_{pp} of 0.4 s. Maximum field values have been $|\vec{H}_x| = 40$ kA/m and $|\vec{H}_z| = 9.6$ kA/m. The rise times Δt_R of the pulses (Fig. 2(a)) are 0.13 s for the H_x and 0.02 s for the H_z field component. The DOWMAT of particles is performed along the $+x$ and $-x$ directions with 100 steps of 5 μm lengths in each direction and the first 100 steps in $+x$-direction. In separate experiments it has been verified that the pulse lengths are sufficient to transport the particles from domain wall to domain wall, i.e., 5 μm per individual pulse. Therefore the average velocity of the particles is 25 μm/s, although the individual particle velocity during a single pulse is higher.[13] The transport direction is defined by the relative phases of $\vec{H}_x$ and $\vec{H}_z$ When alternating $(+\vec{H}_x, +\vec{H}_z)$ and $(-\vec{H}_x, -\vec{H}_z)$ pulses are applied, a movement in $+x$-direction is achieved;

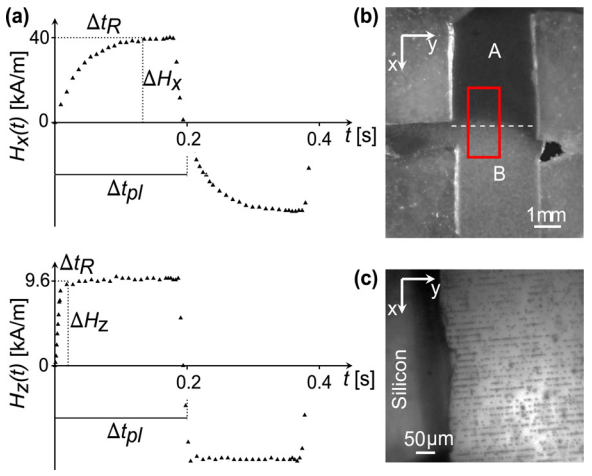

FIG. 2. (a) Measured typical double pulse sequence of H_x and H_z for transport in $+x$-direction with indicated pulse length Δt_{pl} of a single pulse. (b) Photo at the beginning of the experiment: the two fluids A and B with their interface prior to mixing. The analysis area is indicated by the rectangle. (c) Photo of the superparamagnetic bead rows before mixing. During mixing, the bead rows are moved in steps of 5 μm in $\pm x$-directions.

when alternating $(+\vec{H}_x, -\vec{H}_z)$ and $(-\vec{H}_x, +\vec{H}_z)$ pulses are applied, particles are moving in $-x$-direction.[13]

The mixing process is observed by an optical microscope and a video camera through the aperture of the top-coil (see supplementary material[23]). Fluids A and B have been aqueous solutions of spherical PEG-COOH functionalized, superparamagnetic spherical beads with an average diameter of 2.00 ± 0.02 μm determined by dynamic light scattering and a saturation magnetic moment of 4.48×10^{-14} Am^2 obtained in an external magnetic field of 200 kA/m characterized with a vibrating sample magnetometer, purchased from MICROMOD GMBH. Fluid A has been marked by the blue dye *Coomassie Brilliant Blue G-250* and fluid B by *titan yellow* for optical discrimination.

The mixing chamber has been carefully filled with the two fluids via the two injection channels (Fig. 1(b)) avoiding strong mixing during the injection and leading to an almost straight fluid interface. After injection 2 min waiting time ensured that the beads have been trapped in the domain walls' stray fields on the substrate surface. Diffusion based mixing has been observed without bead movement serving as the reference for naturally occurring mixing. Photographs have been taken in regular intervals of 30 s within the first 2 min. During bead transport photographs have been taken each second minute.

Color intensities for fluids A and B have been determined as a function of position in the analysis area of $A = (2.5 \pm 1.2)$ mm^2, corresponding to a fluid volume of 1.5 μL (Fig. 2(b)). They have been correlated to the fluid volume fractions $a(x,t)$ and $b(x,t)$ at positions x within the analysis area at times t by normalizing the color intensities at $x = -\infty$, $t = 0$ to $a(x = -\infty, t = 0) = 1$, $b(x = -\infty, t = 0) = 0$ and at $x = +\infty$, $t = 0$ to $a(x = +\infty, t = 0) = 0$, $b(x = +\infty, t = 0) = 1$, where $x = \pm\infty$ means the farthest distance from the initial fluid interface within the analysis area. The mixing process has then been quantified[5] by describing temporal concentration changes. Volume fractions a and b possessing volume fractions $\bar{a} = a(x, t \to \infty)$ and $\bar{b} = b(x, t \to \infty)$ when both fluids are completely mixed obey the relations

$$a(x,t) + b(x,t) = 1 \forall x, t, \quad \bar{a} + \bar{b} = 1, \tag{1}$$

with

$$\lim_{t\to\infty} a(x,t) = \bar{a} = 0.5 \forall x, \quad \lim_{t\to\infty} b(x,t) = \bar{b} = 0.5 \forall x,$$

in a perfect mixture of completely miscible fluids A and B for $t \to \infty$. With these quantities, the intensity of segregation I can be defined as[5]

$$I(t) = \frac{\sigma_a^2(t)}{\bar{a} \cdot \bar{b}} \equiv \frac{\sigma_b^2(t)}{\bar{a} \cdot \bar{b}} \equiv 4\sigma_a^2(t) \equiv 4\sigma_b^2(t), \tag{2}$$

where $\sigma_a^2(t)$ and $\sigma_b^2(t)$ are the spatial variances of a and b at time t. The two fluids are ideally separated for $I = 1$ and perfectly mixed when $I = 0$.

After color intensity to volume fraction normalization, photographs have been evaluated in the following way: volume fractions $a(x_i, t)$ have been determined at positions (x_i, y_i) in the photographs recorded at defined times t with a sampling distance of $\Delta x = \Delta y = 20\,\mu$m. At each position x_i, averaging has been performed over the full y range in the analysis area. Subsequently, the variances of the volume fractions a and b have been determined according to

$$\sigma_a^2(t) = \frac{1}{n}\sum_{i=1}^{n}[a(x_i,t) - \bar{a}]^2, \sigma_b^2(t) = \frac{1}{n}\sum_{i=1}^{n}[b(x_i,t) - \bar{b}]^2. \tag{3}$$

Intensities of segregation $I(t)$ have then been determined by Eq. (2) as a function of time.

Segregation intensities as functions of time are shown in Figs. 3(a) and 3(b). $I(t=0) \neq 1$ indicates that there is no ideal fluid separation at the start of the different experiments. For the first 2 min with no mixing induced by bead movement, mixing is governed by molecular diffusion, showing a slow decrease of $I(t)$ at an average dI/dt of $-(1.0 \pm 0.2) \cdot 10^{-2}$ min^{-1} (solid line in Fig. 3(a)). Two min after fluid injection, particles had been started to move, 100 steps of 5 μm length in $+x$-direction, followed by 100 steps in $-x$-direction. $I(t)$ decreases rapidly with time (Fig. 3(a)) within a fluid volume of $V = 1.4 \pm 0.1$ μL. This result is remarkable, since the ratio between the mixing chamber height and the bead diameter is 250. However, we cannot exclude that the mixing efficiency is much higher near the boundary layers at the bottom of the fluid chamber, since the lamellae velocity exponentially decreases with increasing container height. Hence, we expect more efficient mixing for smaller height-to-diameter ratios. The decrease of $I(t)$ within the first few minutes of mixing is approximately linear with a slope of $dI/dt = -(3.1 \pm 0.2) \cdot 10^{-2}$ min^{-1} (Fig. 3(a)), three times faster than natural mixing by diffusion. In longer time intervals (Fig. 3(b)), $I(t)$ decreases exponentially for an unaltered movement scheme ($V = 1.8 \pm 0.1$ μL). The linear approximation in Fig. 3(a) corresponds to a first term Taylor series of the overall exponential decay of $I(t)$. Due to Fickian diffusion, dI/dt is expressed in terms of the spatial change of the diffusive flux. Hence, the progress of $I(t)$ originates from the exponential decay of the diffusive flux, i.e., the reduced spatial concentration gradient.

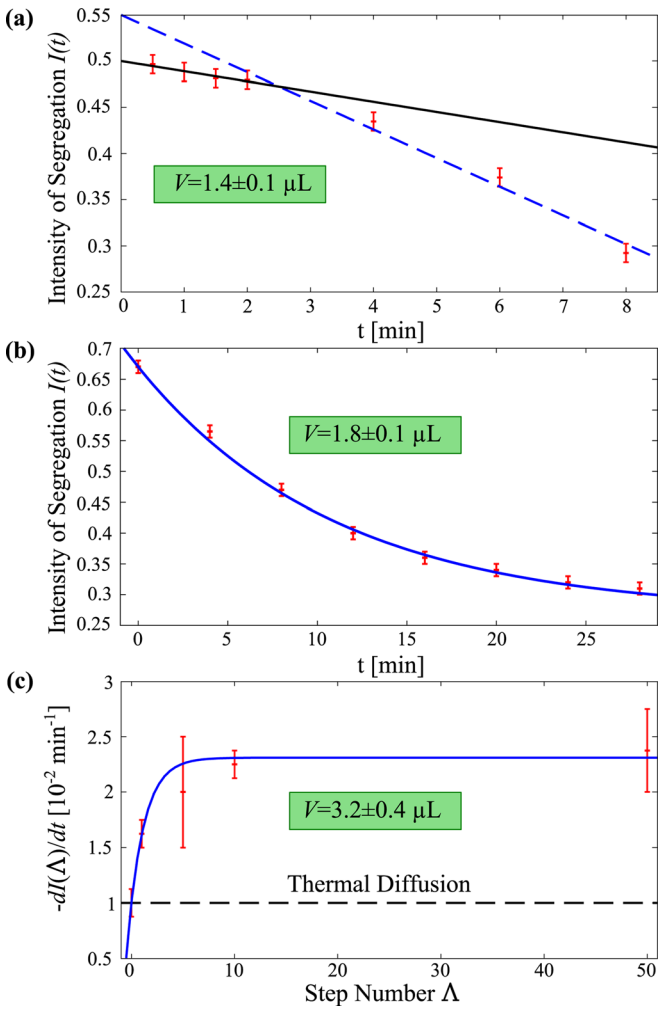

FIG. 3. (a) Intensity of segregation as a function of time for a fluid volume of $V = 1.4 \pm 0.1$ μL. Mixing by particle movement starts after 2 min. Solid line: linear fit of the diffusive regime; dashed line: linear fit during particle movement. (b) Intensity of segregation within a longer time interval for mixing ($V = 1.8 \pm 0.1$ μL). Solid line: fit by an exponential function. (c) Step number dependence of $dI(t)/dt$ for a mean fluid volume of $V = 3.2 \pm 0.4$ μL.

The DOWMAT of the superparamagnetic bead rows on the sample surface cause a movement of the liquid lamellae close to the beads and, at the same time, disturb the adhesion layer of the fluids to the substrate surface. As a consequence, the interface between the fluids and their movability is increased and correspondingly the mixing efficiency. The mixing speed (linear approximation as in Fig. 3(a)) as a function of successive steps in one direction is shown in Fig. 3(c) for individual pulse times of 500 ms within a mean fluid volume of $V = 3.2 \pm 0.4$ μL. The mixing speed increases dramatically for relatively small numbers of steps and saturates already for about 10 steps forward/backward.

In summary, we have proven a technique for microfluid mixing, based on DOWMAT of full superparamagnetic bead rows on the surface of an exchange bias layer system artificially patterned into parallel-stripe magnetic domains with no additional measures for surface coating. The proof of a considerably increased mixing speed holds promise that this technique can be efficiently integrated in microfluidic devices or used with microwell plates.

We gratefully acknowledge Singulus Technologies AG producing the EB layer systems and the BMWi (03VWP0006) for financial support.

[1]C. Ahn and J.-W. Choi, *Springer Handbook of Nanotechnology* (Springer, Berlin, 2007), pp. 523–548.
[2]K. Jensen, Chem. Eng. Sci. **56**, 2 (2001).
[3]A. Manz, N. Graber, and H. M. Widmer, Sens. Actuators, B **1**, 244 (1990).
[4]H. A. Stone and S. Kim, AIChE J. **47**, 1250 (2001).
[5]P. Danckwerts, Appl. Sci. Res. **3**, 279 (1952).
[6]J. Ottino and S. Wiggins, Philos. Trans. R. Soc. London, Ser. A **362**, 923 (2004).
[7]V. Hessel, H. Löwe, and F. Schönfeld, Chem. Eng. Sci. **60**, 2479 (2005).
[8]K. Ryu, K. Shaikh, E. Goluch, Z. Fan, and C. Liu, Lab Chip **4**, 608 (2004).
[9]R. Miyake, T. Lammerink, M. Elwenspoek, and J. H. J. Fluitman, in *Proceedings IEEE MEMS Workshop* (Ft. Lauderdale, FL, 1993), p. 248.
[10]M. A. M. Gijs, Microfluid. Nanofluid. **1**, 22 (2004).
[11]P. Tierno, T. H. Johansen, and T. M. Fischer, J. Phys. Chem. B **111**, 3077 (2007).

[12]C. Liu, L. Lagae, R. Wirix-Speetjens, and G. Borghs, J. Appl. Phys. **101**, 024913 (2007).
[13]A. Ehresmann, D. Lengemann, T. Weis, A. Albrecht, J. Langfahl-Klabes, F. Göllner, and D. Engel, Adv. Mater. **23**, 5568 (2011).
[14]C. Liu, L. Lagae, and G. Borghs, Appl. Phys. Lett. **90**, 184109 (2007).
[15]L. E. Helseth, T. M. Fischer, and T. H. Johansen, Phys. Rev. E **67**, 1 (2003).
[16]L. E. Johansson, K. Gunnarsson, S. Bijelovic, K. Eriksson, A. Surpi, E. Göthelid, P. Svedlindh, and S. Oscarsson, Lab Chip **10**, 654 (2010).
[17]M. Donolato, P. Vavassori, M. Gobbi, M. Deryabina, M. F. Hansen, V. Metlushko, B. Ilic, M. Cantoni, D. Petti, S. Brivio, and R. Bertacco, Adv. Mater. **22**, 2706 (2010).
[18]A. Ehresmann, *Recent Res. Dev. Appl. Phys.* (Trivandrum, 2004), Vol. 7 part II, pp. 401–402.
[19]A. Ehresmann, D. Engel, T. Weis, A. Schindler, D. Junk, J. Schmalhorst, V. Höink, M. D. Sacher, and G. Reiss, Phys. Status Solidi B **243**, 29 (2006).
[20]A. Ehresmann, I. Krug, A. Kronenberger, A. Ehlers, and D. Engel, J. Magn. Magn. Mater. **280**, 369 (2004).
[21]D. Rugar, H. J. Mamin, P. Guethner, S. E. Lambert, J. E. Stern, I. McFadyen, and T. Yogi, J. Appl. Phys. **68**, 1169 (1990).
[22]I. Ennen, V. Höink, A. Weddemann, A. Hütten, J. Schmalhorst, G. Reiss, C. Waltenberg, P. Jutzi, T. Weis, D. Engel, and A. Ehresmann, J. Appl. Phys. **102**, 013910 (2007).
[23]See supplementary material at http://dx.doi.org/10.1063/1.3701723 for the DOWMAT of superparamagnetic bead rows.